

## Original Article

# Study of trabecular bone fracture healing in a rabbit model

Yang Zhao<sup>1\*</sup>, Siwen Yang<sup>2\*</sup>, Guanghong Wang<sup>1</sup>

<sup>1</sup>Department of Orthopaedics, Harbin 242 Hospital, Harbin 150000, Heilongjiang, China; <sup>2</sup>Harbin Medical University Cancer Hospital, Harbin 150000, Heilongjiang, China. \*Equal contributors and co-first authors.

Received November 19, 2017; Accepted May 3, 2018; Epub August 15, 2018; Published August 30, 2018

**Abstract:** Clinically, fractures in metaphysis cancellous bones heal in a much more rapid fashion and have several unique features when compared with diaphyseal cortical bone fractures. According to their specific anatomical features, we hypothesized that traditional staging of cortical bone healing may not apply to the diaphyseal cancellous bone fracture healing process. The aim of the current study was to investigate the unique healing processes of trabecular fracture and summarize a new staging system specialized for metaphysis cancellous bone fracture, which will lead to new comprehension and treatment for metaphysis cancellous bone fracture. In this study, a new metaphysis cancellous bone fracture model of the proximal tibia in rabbits was established according to the principle of complete anatomical reduction, rigid internal fixation, and sufficient blood supply. The model was quantified to identify the pathophysiology and morphology of the healing process after fracture in the hope of finding experimental support for understanding the healing pattern of metaphysis cancellous bone fracture. The whole fracture healing process of trabecular bone can be divided into four stages by histology: the first was characterized by cellular activation and differentiation from immediately after surgery to 3 weeks; the second was characterized by the formation of woven bone or new trabeculae from 5 days to 4 weeks; the third was the transformation of newly formed woven bone into a lamellar structure from 9 days to 6 weeks; the fourth was the period of remodeling after 2 weeks and reached a peak at 6 weeks. There was no obvious fibrous tissue or chondrification formed during the entire healing process. The data of bone histomorphometry and biomechanical analysis showed structural parameters and parameters of healing strength changed as a unimodal curve. Our data demonstrate that the metaphysis cancellous fracture heals in a unique fashion, which can be divided into four histological stages. It differs from cortical fracture healing. Histological analysis showed that the fracture healed directly through intramembranous repair and included two different patterns: one occurred in the marrow of the fracture site, and the other occurred on the surface of pre-existing trabeculae.

**Keywords:** Cancellous bone fracture healing, novel staging system

### Introduction

Fractures of extremities are mainly fractures of trabecular bones [1-4]. Clinically, fractures in the extremities or cancellous bone heal in a much more rapid fashion and have several unique features when compared with diaphyseal fractures. For example, distal radial fracture and lateral malleolus fracture will heal directly without callus formation under conditions of anatomical reduction and rigid internal fixation. This pattern of fracture healing has been called "primary healing". Although numerous studies using various animal models have been performed on fracture healing and treatment, most address the diaphyseal fracture of

long bones [5]. The healing processes of periarticular cancellous bone fractures have not been well investigated.

The mechanism of diaphyseal fracture healing is a complex, multi-step process, in which the periosteum plays a pivotal role. Intramembranous and endochondral ossifications combine to complete this healing process [6, 7]. Compared with the majority of diaphyseal fractures, trabecular bone fractures recover through a unique healing process [4]. Charnley and Baker observed that the woven bone trabeculae soon increased in thickness by surface deposition of new bone matrix [8]. Uthoff and Rahn showed similar findings in various models (rats, rabbits

## Unique four stage healing pattern in cancellous fracture healing

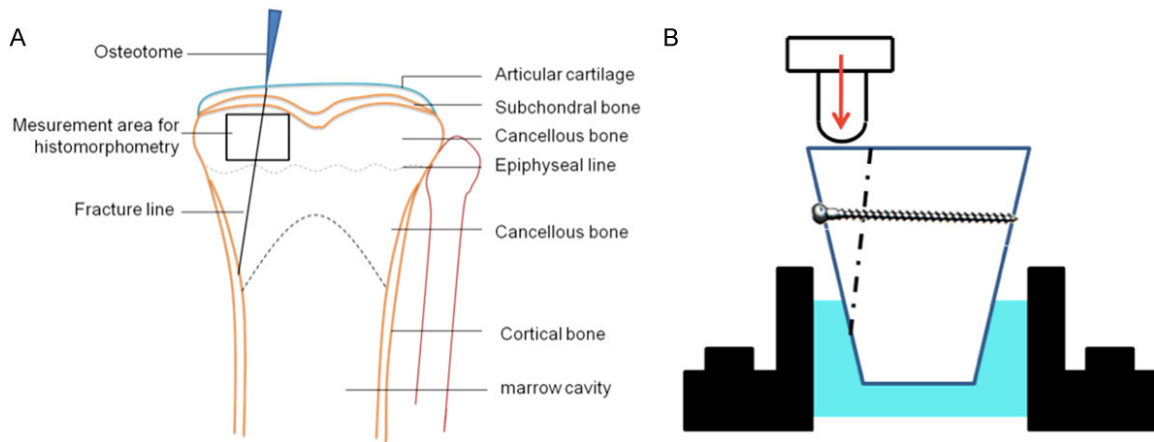


**Figure 1.** A. Diagram of the rabbit proximal tibia and osteotomy. The rectangular region is the measurement area for bone histomorphometry. B. Diagram of biomechanical analysis.

and dogs). As long as the fractures were not displaced and trabeculae were properly lined with osteoblasts, no internal cartilage formation or periosteal callus was observed [9, 10]. Although much effort has been made by these previous studies, there are still many obstacles to reveal these issues. For examples, in these previous studies an oscillating saw was used to make the osteotomies where a gap was formed at the fracture site and local high temperature from the oscillating saw cutting may cause osteonecrosis, both of which interfered with the reduction and brought difficulties in healing.

In this study, a new metaphysis cancellous bone fracture model at the proximal tibia of the rabbit was established according to the principle of complete anatomical reduction, rigid internal fixation, and protection of the blood supply. The model was quantified to identify the pathophysiology and morphology of the healing process after fracture in the hope of finding experimental support for understanding the healing pattern of metaphysis cancellous bone fracture. The aim of our study is to reveal the healing processes of trabecular fracture and summarize a new staging system specialized for metaphysis cancellous bone fracture. Our data demonstrate the unique healing process of trabecular bone fracture, which is distinct from that of cortical bone fractures. Clinically, this finding will lead to a more specialized comprehension of the healing process of metaphysis cancellous bone fracture and will promote the development of new therapies.

## Material and methods

### Animal model

This study was carried out according to the guidelines of the Animal Ethics Committee of the Peking University Health Science Center. Sixty 6-month-old New Zealand white rabbits provided by Peking University People's Hospital were used in the study. The animals were divided into 11 groups with 5 animals in each group. The animals were anesthetized with sodium pentobarbital through the auricular vein.

A 2-cm longitudinal skin incision was made medial to the knee joint. The joint capsule was cut open, disclosing the medial tibial plateau. An osteotomy with a sagittal blade was performed on the medial tibial plateau at the attachment point of the medial meniscus anterior horn directly, resulting in the cleavage fracture of the medial tibial plateau (AO classification, B1), and then the fracture fragment was reduced *in situ*. The size of the fragment was about 0.5 cm × 1 cm × 1.5 cm. The fracture line was in a parasagittal plane. The osteotomy site was then fixed with single cancellous bone screw at the anterior border of attachment point of the medial collateral ligament (**Figure 1A**).

After surgery, the animals were returned to their individual cages for recovery and allowed to move freely. At 1, 3, 5, 7, 9, 11, and 14 days and 3, 4, 6, and 8 weeks postoperatively, the

## Unique four stage healing pattern in cancellous fracture healing

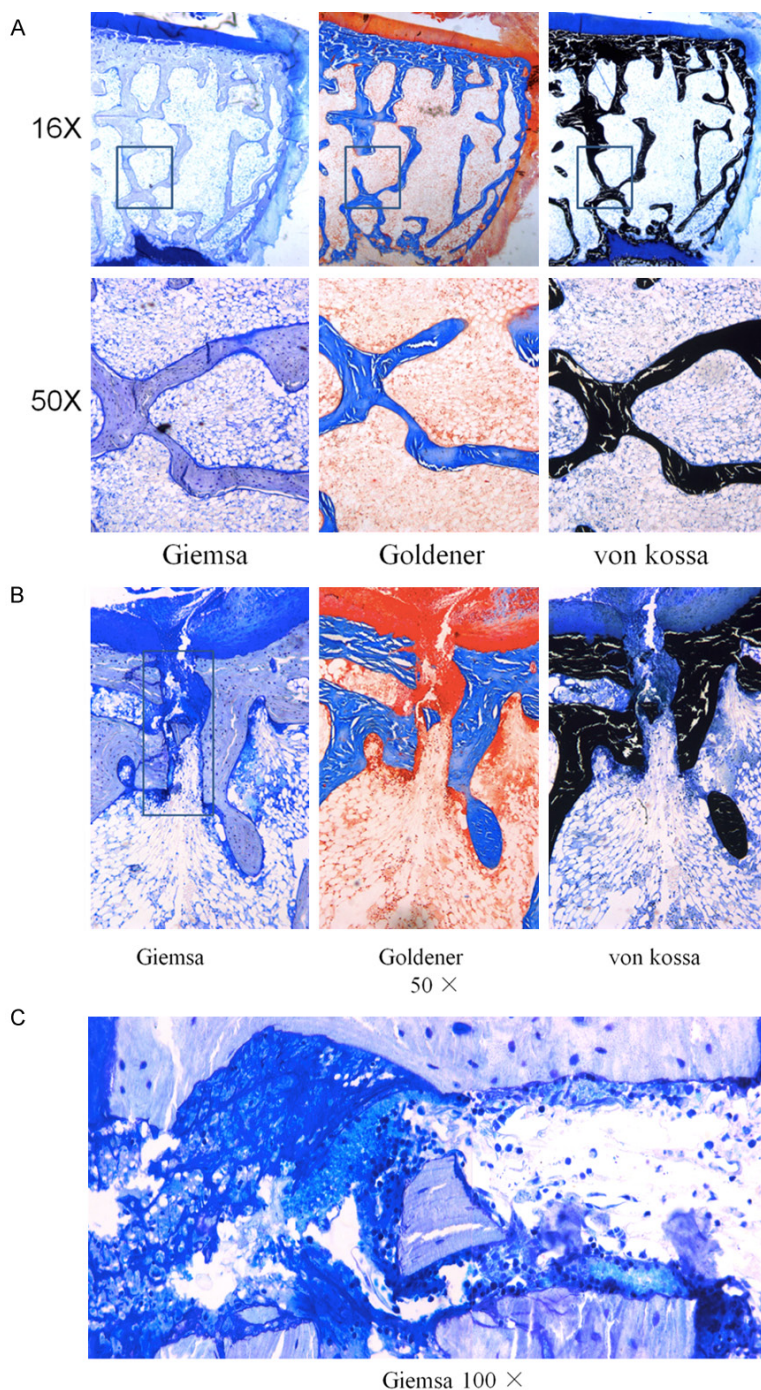


**Figure 2.** A. Normal structure of proximal end tibia of rabbits (Giemsa, Goldmer and von Kossa stain, undecalcified section). B. Histological features of the fracture site at 1 day after surgery. The normal structure was disrupted and gained reduction *in situ*. C. A limited hemorrhage could be seen in the fracture gap near the subchondral bone (undecalcified, Giemsa stain, 100 times amplification).

animals were sacrificed with an overdose of sodium pentobarbital. Conventional X-ray radiograms of the bilateral tibiae were taken after the animals had been sacrificed. The bilateral tibiae were then harvested and fixed with 10%

formalin for histologic studies or stored under the condition of  $-200^{\circ}\text{C}$  for biomechanical testing.

### Section preparation

The proximal parts of the tibiae were fixed with 70% ethanol, then dehydrated in ascending grades of ethanol, defatted in dimethyl benzene, and embedded in methyl methacrylate without decalcification. Undecalcified  $5\ \mu\text{m}$  sections were prepared using a Jung-K microtome (Reichert-Jung, Heidelberg, Germany). The sections were stained in Giemsa, von Kossa and Masson-Goldner techniques

### Bone histomorphometry

Nomenclature, symbols, and units used in bone histomorphometry were well described in the previous study [11, 12]. In our study, the following parameters were examined using a semi-automatic digitizing system for bone histomorphometry (Leica QWin, Leica, Germany), with final magnification of  $50\times$ : trabecular bone volume (bone volume/tissue volume, BV/TV), trabecular thickness (Tb.Th), trabecular number (Tb.N) and trabecular separation (Tb.Sp). The areas measured were defined by a rectangular region in the cancellous bone between the subchondral bone and epiphyseal line for 2 mm on either side of the fracture midline (**Figure 1A**).

### Biomechanical testing

The samples for biomechanical testing were divided into three groups: with fixation, without fixation, and the control group. The time points were 1, 2, 3, 4, 6, and 8 weeks postoperatively. The vertical compression test detected biomechanical changes during the fracture healing including

## Unique four stage healing pattern in cancellous fracture healing

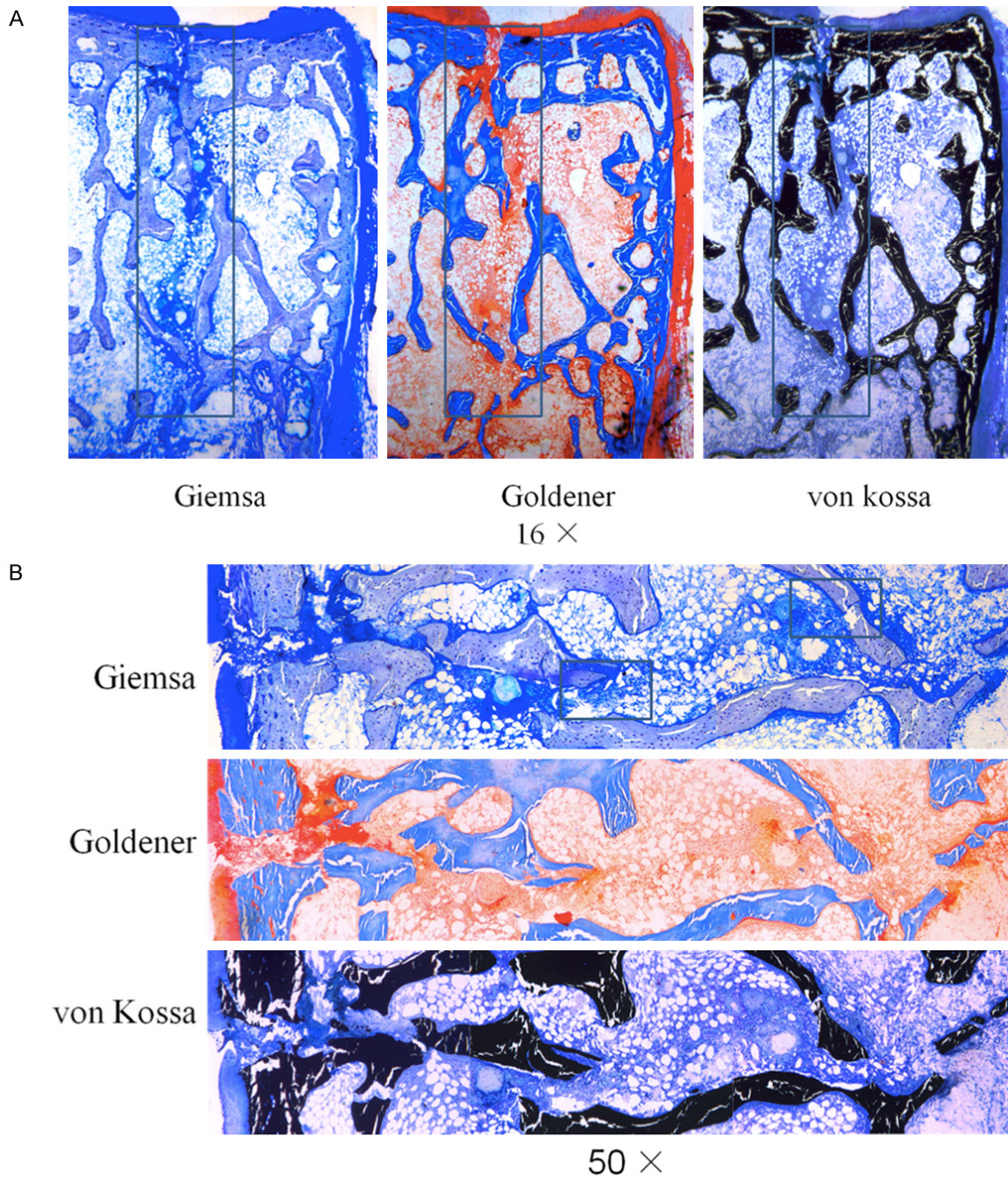


**Figure 3.** A. Histological features of the fracture site at 3 days after surgery. B. Cellular proliferation was activated at the fracture site. The places where the cellular proliferation occurred included the marrow intertrabecular region and the surface of pre-existing trabeculae. The cells were spindle or polygonal, and retained mesenchymal cell appearance.

the maximum load and maximum energy absorption (**Figure 1B**).

### *Statistical analysis*

Descriptive statistics of all variables are presented as means  $\pm$  SD. Comparisons between

different time points were evaluated by performing analysis of variance (ANOVA). ANOVA was employed for statistical comparison of the mean value of the structural and biomechanical parameters of trabecular bone samples from various time points. There are five animals in each group.

## Unique four stage healing pattern in cancellous fracture healing

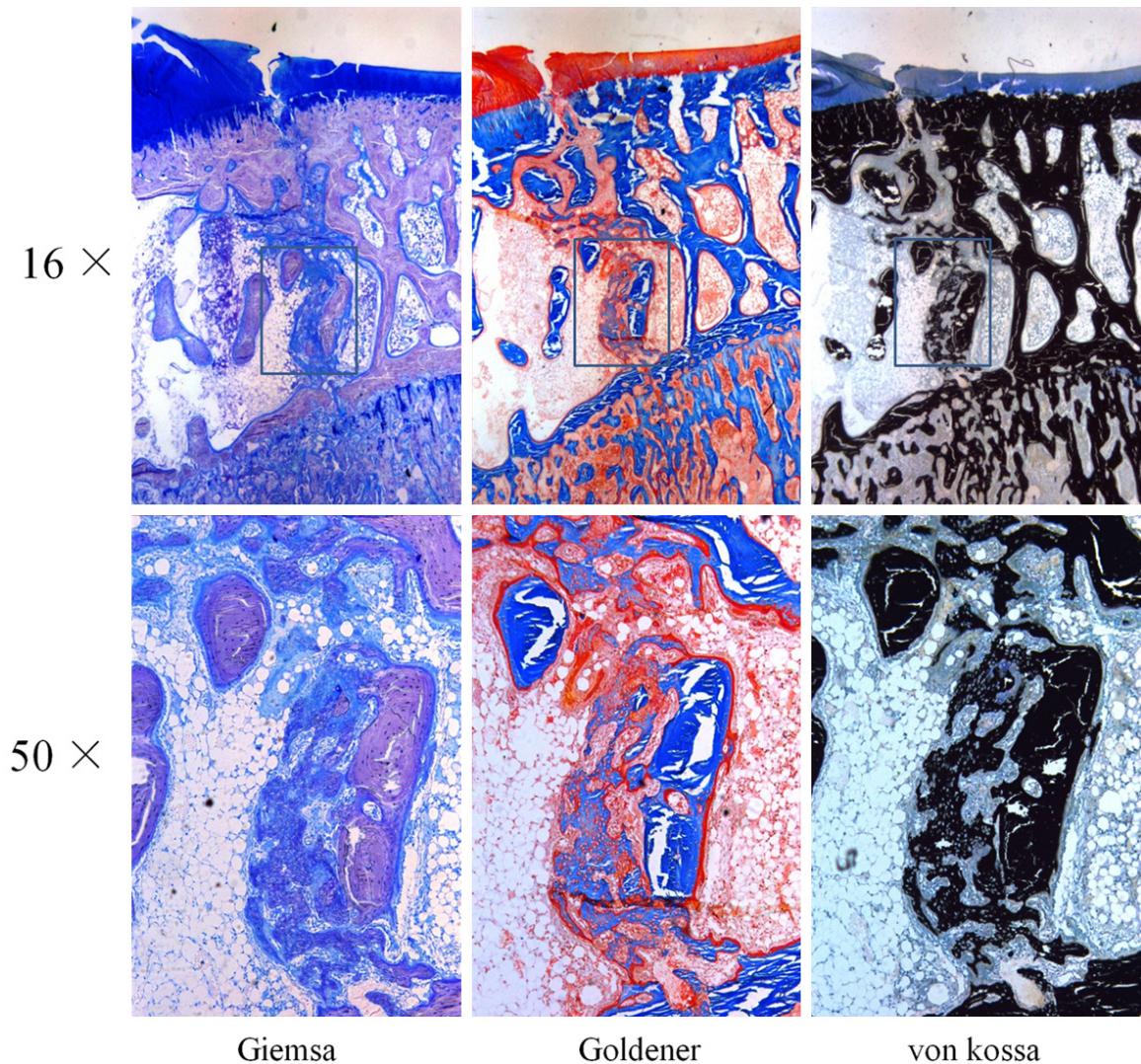


**Figure 4.** Histological features of the fracture site at 7 days after surgery. There were a large number of woven bones formed at the fracture site. The osteoid continued to form. Von Kossa stain showed mineralization of the osteoid and woven bone in good condition.

ANOVA analysis was used to determine factors predicting trabecular bone healing measured by histomorphometry and maximum load and energy absorption by biomechanical testing. The ANOVA model analyzed the following variables: bone volume/tissue volume, trabecular number, trabecular thickness, trabecular separation, maximum load, and energy absorption. The limit of significance was set at  $p < 0.05$  for all analyses. Post-hoc test with Fisher's protected least significant difference (PLSD) was employed to compare the differences between two groups. All statistical analyses were carried out using SPSS for Windows version 14.

### Results

#### *Results of histological observation*

At 1 day after surgery, the structure of the epiphysis was broken and a limited hemorrhage could be found at the area near to the subchondral bone. No obvious hematoma had formed at the whole fracture site (**Figure 2A-C**). At 3 days after surgery, there were numerous cells within the fracture site. The cells were mesenchymal stem cells, which could be distinguished from the cell's morphology and would differentiate into osteoblasts with time. The matrix intercellular structure is similar as in

## Unique four stage healing pattern in cancellous fracture healing

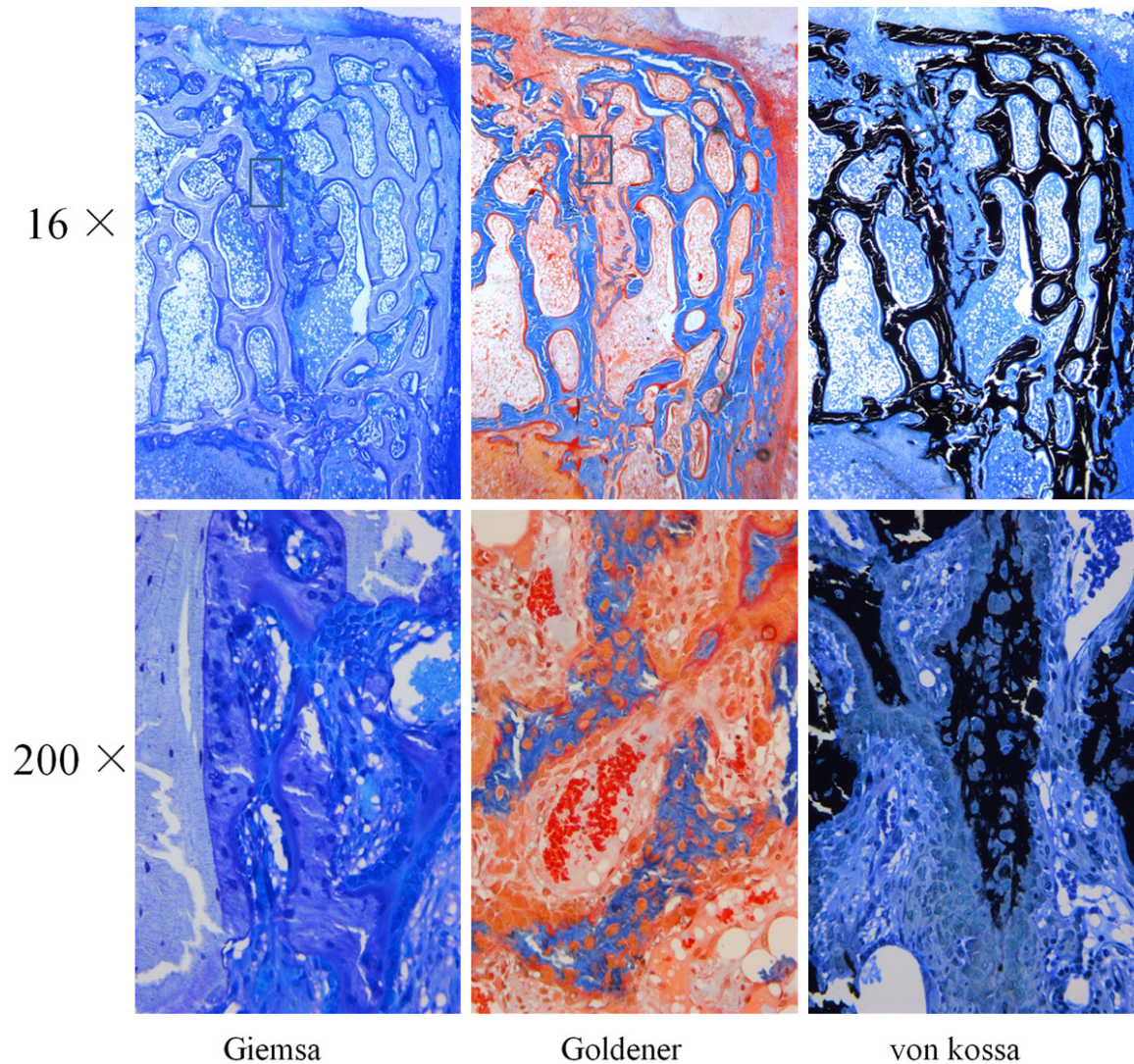


**Figure 5.** Histological features of the fracture site at 9 days after surgery. The degree of cell proliferation and the woven bone formation began to decrease compare with the previous time point. Cubic osteoblasts with neater arrangement appeared on the surface of newly formed woven bone and began to secrete osteoid.

fibrous cords. The activated mesenchymal osteoblasts proliferated and secreted high amounts of collagen to form the osteoid. The osteoblasts, which differentiated from osteoprogenitor cells, on the original trabecular bone surface activated significantly and secreted osteoid. It is the most active at the fracture gap center, waning to both sides (**Figure 3A, 3B**). At 5 days after surgery, the cellular proliferation continued to intensify and formed the primary woven bone. This newly formed woven bone was like a short branch and mainly existed around the pre-existing trabeculae even at the surface of fragments. There were large amounts of osteoid around this newly formed woven bone, indicating that the formation of

woven bone continued. At 7 days after surgery, the amount of the woven bone increased at the fracture site with the orientation of the matrix still random (**Figure 4**). There were two different patterns of bone formation that could be observed at this time point. One was based on the pre-existing trabeculae to form the lamellar bone, directly resulting in the increase of size of the pre-existing trabeculae, while the other was the woven bone formed at the medulla of the fracture site like an island to connect both sides of the fracture. At 9 days after surgery, the cell proliferation and the formation of the woven bone decreased. The woven structure in the fracture site began to be replaced by a more orderly arranged lamellar structure,

## Unique four stage healing pattern in cancellous fracture healing

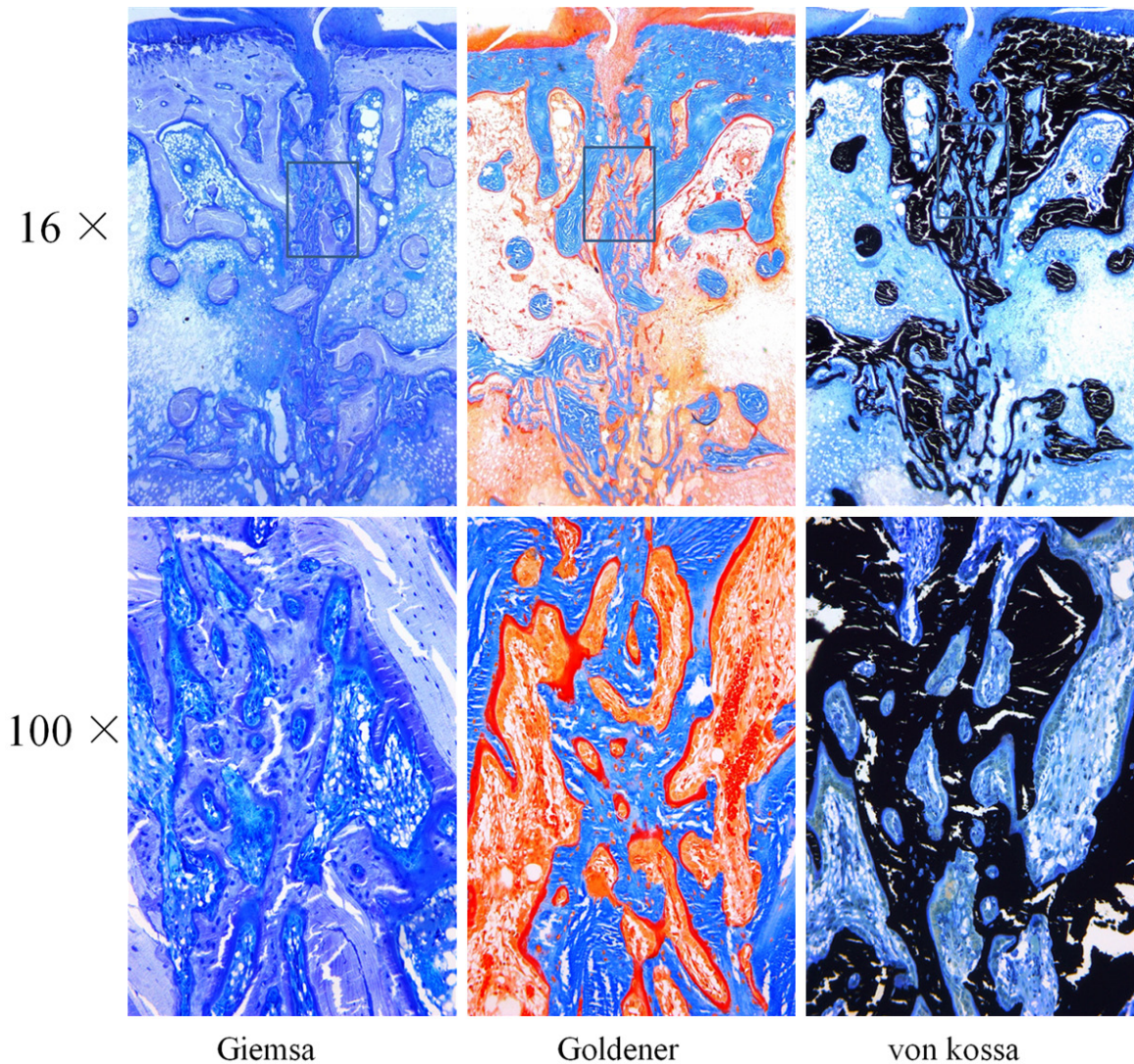


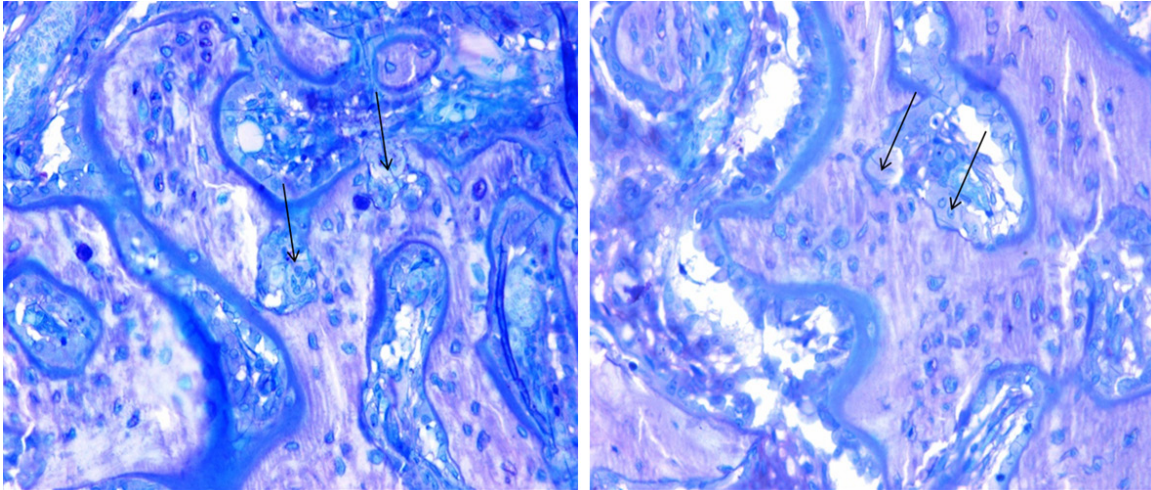
**Figure 6.** Histological features of the fracture site at 11 days after surgery. It could be observed that there were numerous newly formed trabecular bones within the fracture site with high density and which connected the fragments together like a net. The osteoblasts on these newly formed trabecular bones began to form the lamellar structure to thicken the size.

with higher density and consistent distribution compared with previous time points. The new trabecular bone mineralized well and formed the initial grid structure, but had not transformed into the typical lamellar structure yet (**Figure 5**).

At 11 days after surgery, these newly formed trabecular bones became more mineralized and connected. The size of the newly formed trabecular bone and pre-existing trabeculae was significantly larger than that of previous time points after surgery (**Figure 6**). At 2 weeks after surgery, the fracture site was fully filled with newly formed trabeculae. The relatively

typical lamellar structure could be seen on the surface of the newly formed trabecular bone. Another feature of this time point was the osteoclast, which appeared and formed lacunae on the surface of newly formed trabecular bone. It symbolized the beginning of the bone remodeling (**Figure 7**). At 3 weeks after surgery, cell proliferation was finished. Barely any new woven bone could be seen in the wound. Most newly formed trabecular bone mineralized well and had formed the typical lamellar structure. At 4 weeks after surgery, the basic multi-cellular unit (BMU) appeared on the surface of almost all the newly formed trabecular bone at the fracture site (**Figure 8A, 8B**), which

## Unique four stage healing pattern in cancellous fracture healing



Giemsa 200 ×

**Figure 7.** Histological features of the fracture site at 2 weeks after surgery. The newly formed trabecular bone was bigger and the connection better than the previous time point because of the lamellar bone formation. Arrows show the osteoclasts and absorption lacunae on the surface of newly formed trabecular bone (Giemsa stain, 200 times amplification).

indicated that the bone remodeling was activated. Remodeling activity peaked at 6 weeks after surgery (**Figure 9A, 9B**). By 8 weeks, the normal trabecular structure has been restored in the wound (**Figure 10**).

### *Measurement of proportion of cancellous bone and statistical analysis*

The total volume of the new-formed trabeculae (woven bone) and pre-existing trabecular bone was measured. The trabecular bone volume (bone volume/tissue volume, BV/TV) and trabecular number (Tb.N) reached a peak at 2 weeks then decreased. The trabecular separation was smallest at 2 weeks, while the trabecular thickness continued to increase (**Table 1**).

### *Biomechanics determination*

The results of biomechanical testing showed that the maximum load and the absorbing energy were lowest at 1 week after surgery and reached or exceeded the normal level at 2 weeks after surgery. Both the maximum load and the absorbing energy kept increasing before 4 weeks and reached a peak at 4 weeks after surgery, then decreased after that but were still higher than the normal level (**Table 2**).

### **Discussion**

For modern orthopedic surgery, the main principles for treating fractures of extremities are anatomical reduction, rigid internal fixation, and protection of the blood supply in the clinic [13-15]. In this study a new extremity fracture model was performed under the conditions of anatomical reduction and rigid internal fixation at the proximal bilateral tibia of the rabbit. This model provides a new means of studying the fracture healing process in cancellous bone of the proximal tibia with, for the first time, quantitative analysis for histology.

Recently, several novel improvements have been made in fracture healing research. Duan reported that VEGF gene transfer into MSCs enhances bone repair *in vivo* by promoting vascularization [16]. In support of this finding, Senel reported that circulating VEGF concentrations were decreased in post-menopause osteoporosis patients and VEGF may play an important role in bone health [17]. Moreover, Ishikawa' team discovered that MCP-1/CCR2 signaling in the periosteum and endosteum is essential for the recruitment of mesenchymal progenitor cells in the early phase of fracture healing [18]. In addition, Kawakami and colleagues demonstrated that the EPC SDF-1/

## Unique four stage healing pattern in cancellous fracture healing

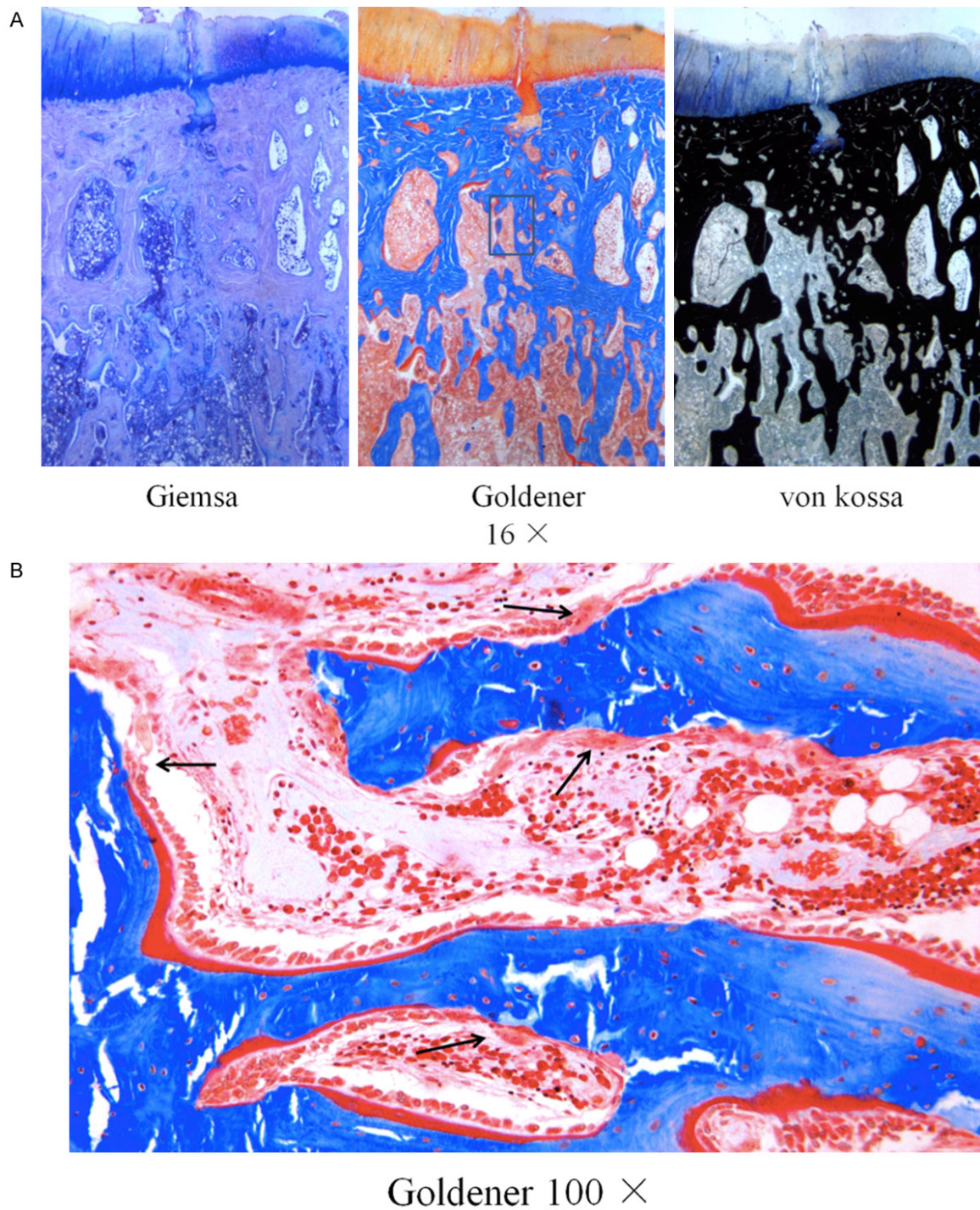


**Figure 8.** Histological features of the fracture site at 4 weeks after surgery. A. No obvious cell proliferation or woven bone formation could be observed at this time. B. Arrows show the basic multicellular unit (BMU) on the surface of newly formed trabecular bones.

CXCR4 axis plays an important role in bone fracture healing [19]. However, most of the previous studies employed focused on cortical fractures and little was specified within the scope of cancellous bone fracture.

Although numerous previous studies have investigated diaphyseal fracture healing, the healing process of cancellous bone after peri-articular fracture has not received enough attention [5, 20]. Jarry and Uthoff compared

## Unique four stage healing pattern in cancellous fracture healing

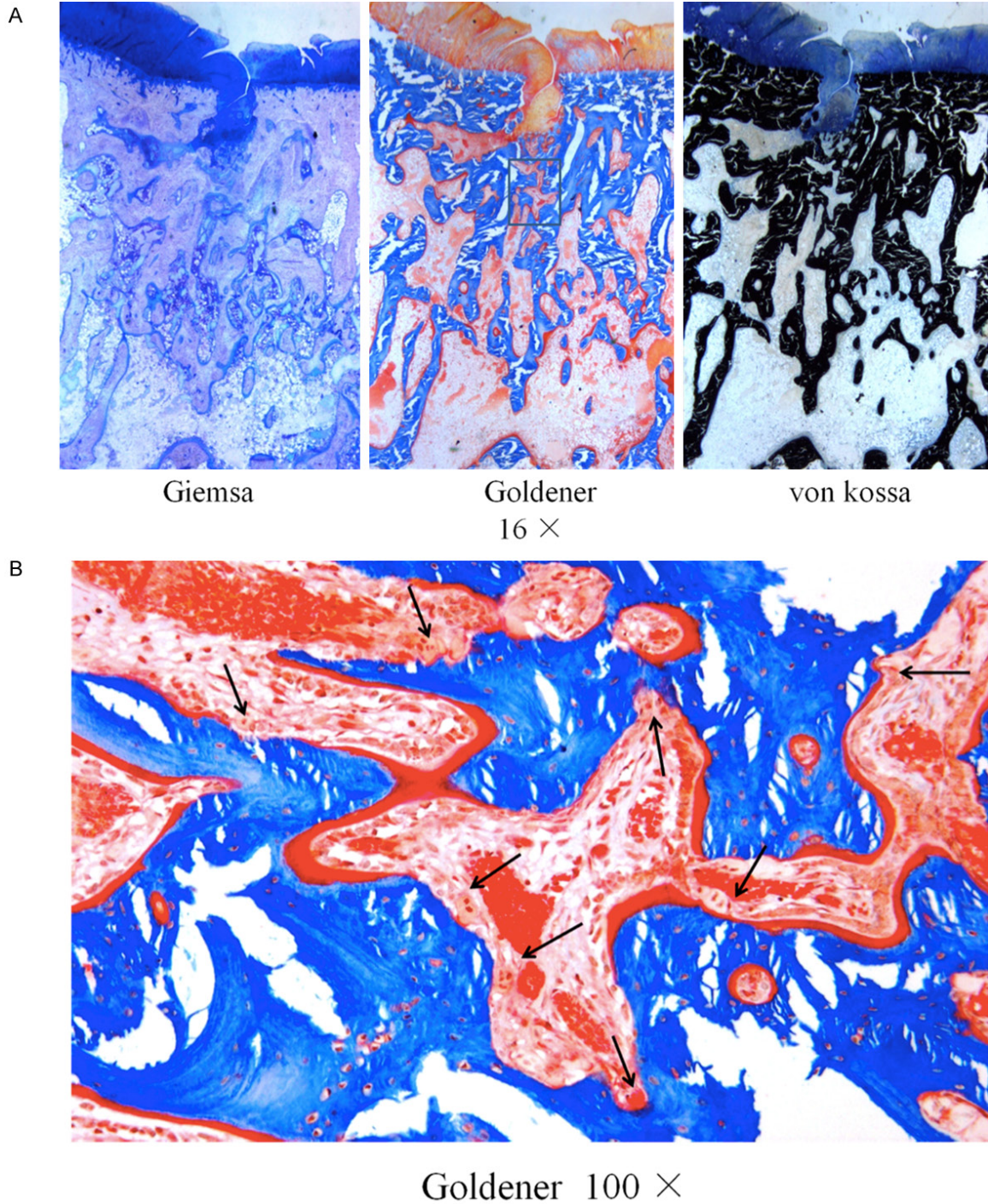


**Figure 9.** Histological features of the fracture site at 6 weeks after surgery. A. The density of trabecular bone seemed lower than 4 weeks. B. Arrows show the basic multicellular unit (BMU) on the surface of almost all newly formed trabecular bones. The number of BMU was higher than 4 weeks after surgery. It meant that the activity of bone remodeling reached the peak at this time point.

stable and unstable situations in a metaphyseal fracture-healing model in rats, rabbits, and dogs. Under stable conditions, direct trabecular healing occurred based on the pre-

existing trabecular bone, and under unstable conditions fibrous tissue was formed initially then the woven bone formed. In both situations no significant callus formation was observed

## Unique four stage healing pattern in cancellous fracture healing

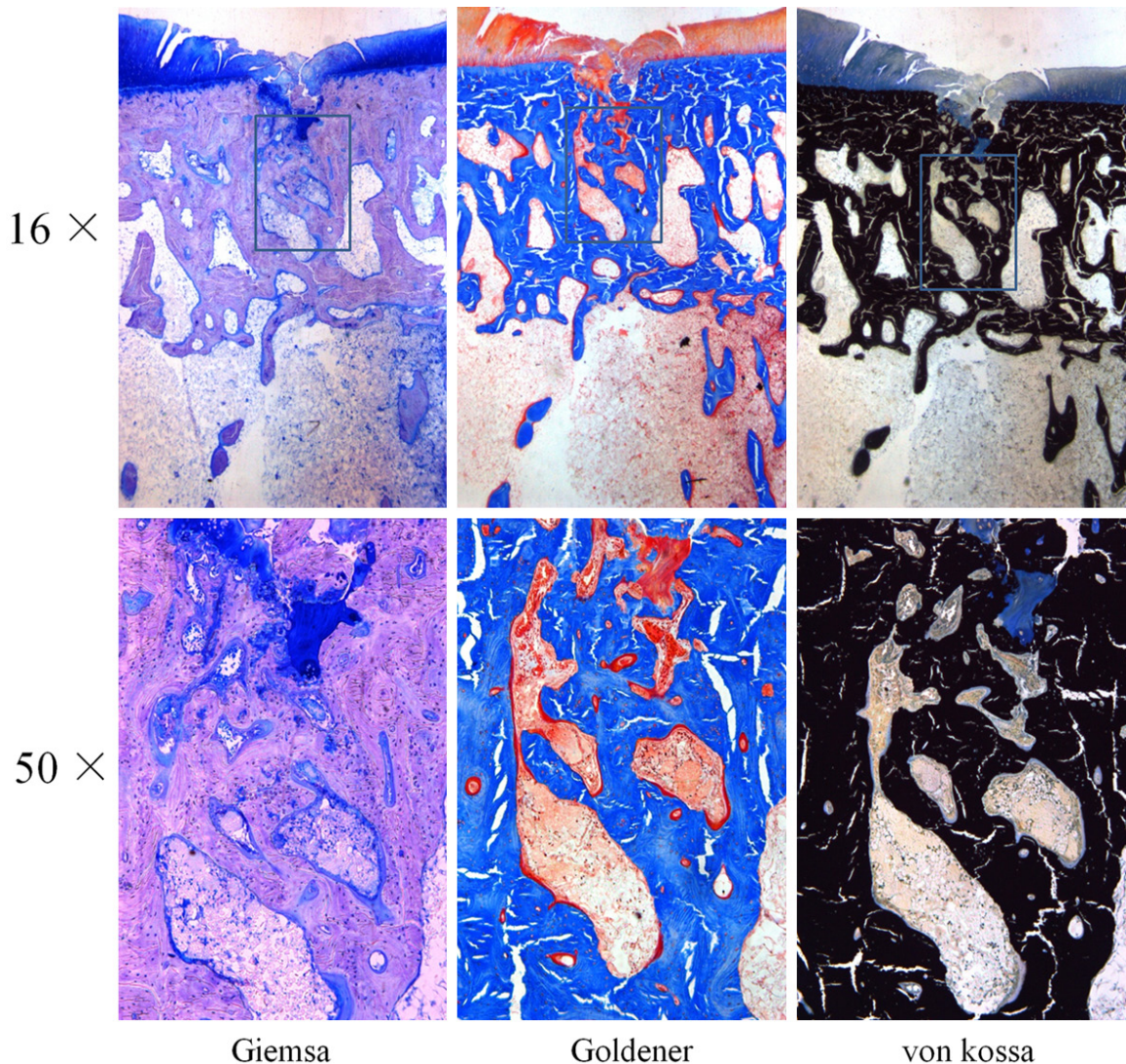


**Figure 10.** Histological features of the fracture site at 8 weeks after surgery. The activity of bone remodeling had significantly decreased and the structure of the fracture site showed no obvious difference from the normal structure.

[9,10]. Fractures were created using an oscillating saw or by manual means which resulted in extensive damage to the bone structure. In the aspect of internal fixation they used Kirschner wire for stable fracture and no fixation for unstable fracture. According to the modern clinical principle their animal fracture model had no stability. Claes developed a new animal model in 2009 that made the metaphyseal fracture of the distal femur in the goat in order to study the effect of the biomechanical environment on the histology during the process of fracture healing. For their animal model, they made a gap at the fracture site for a special purpose, which disagreed with modern clinical practice. Unlike in Uthoff study, we

used a blade to split the fragment off. The direction of osteotomy was parallel with the line of force. After fracture the reduction was performed *in situ* at once and fixed with a cancellous screw. These methods protected the bone tissue from severe damage and ensured the stability of the fracture. We chose a rabbit model to conduct the current study because we found it difficult to secure a stable cancellous fracture a fixation on a smaller animal model such as mouse or rat. Moreover, we used the osteotomy to mimic the typical clinical cancellous fracture. Additionally, the osteotomy we designed enabled sufficient fixation and made it easy to conduct a biomechanical test.

## Unique four stage healing pattern in cancellous fracture healing

**Table 1.** Structural parameters of trabecular bones in healing process measured by histomorphometry including newly formed and pre-existing trabecular bone (mean  $\pm$  SD)

Time	BV/TV (%)	Tb.N (#/m <sup>2</sup> )	Tb.Th [ $\mu$ m]	Tb.Sp [ $\mu$ m]
1 w	32.34 $\pm$ 6.04	2.33 $\pm$ 0.58	144.32 $\pm$ 38.64	310.24 $\pm$ 93.39
2 w	44.48 $\pm$ 9.27	2.93 $\pm$ 0.65	154.42 $\pm$ 29.46	200.26 $\pm$ 65.86
3 w	33.99 $\pm$ 12.07	2.16 $\pm$ 0.65	162.77 $\pm$ 48.66	347.46 $\pm$ 189.88
4 w	31.82 $\pm$ 3.51	1.71 $\pm$ 0.42	191.17 $\pm$ 31.59	420.04 $\pm$ 125.27
6 w	25.34 $\pm$ 2.82	1.40 $\pm$ 0.16	182.68 $\pm$ 31.17	536.98 $\pm$ 59.15
8 w	29.27 $\pm$ 2.96	1.47 $\pm$ 0.02	198.34 $\pm$ 23.60	478.44 $\pm$ 11.05

BV/TV: 2 w vs. 3 w,  $p < 0.05$ ; 2 w vs. 1 w, 6 w, 8 w,  $p < 0.01$ ; TB.N: 2 w vs. 1 w, 3 w,  $p < 0.05$ ; 2 w vs. 4 w, 6 w, 8 w  $p < 0.01$ ; Tb.Sp: 2 w vs. 3 w,  $p < 0.05$ ; 2 w vs. 4 w, 6 w, 8 w,  $p < 0.01$ ; Tb.Th: 1 w vs. 4 w, 8 w,  $p < 0.05$ .

**Table 2.** Maximum load and maximum energy absorption of fracture site at different times postoperatively (mean  $\pm$  SD)

	Maximum load (N)		Maximum energy absorption (J)	
	Without screw	With screw	Without screw	With screw
Control	633.98 $\pm$ 62.20		0.65 $\pm$ 0.17	
Immediately		455.00 $\pm$ 137.01		0.53 $\pm$ 0.27
1 w	222.96 $\pm$ 10.78 <sup>a</sup>	559.21 $\pm$ 157.63	0.34 $\pm$ 0.28 <sup>a</sup>	0.84 $\pm$ 0.25 <sup>a</sup>
2 w	546.12 $\pm$ 125.85	669.37 $\pm$ 137.51	0.61 $\pm$ 0.18	1.38 $\pm$ 0.55
3 w	491.12 $\pm$ 106.63	703.97 $\pm$ 71.92	0.80 $\pm$ 0.41	1.34 $\pm$ 0.39
4 w	684.89 $\pm$ 86.34 <sup>aa</sup>	744.68 $\pm$ 78.02	0.99 $\pm$ 0.32 <sup>aa</sup>	2.05 $\pm$ 0.43 <sup>aa</sup>
6 w	545.15 $\pm$ 194.11	653.67 $\pm$ 148.40	0.79 $\pm$ 0.19	0.69 $\pm$ 0.27
8 w	568.97 $\pm$ 101.28	675.31 $\pm$ 75.66	0.85 $\pm$ 0.47	1.10 $\pm$ 0.68

<sup>a</sup>1 w vs. other groups,  $p < 0.05$ ; <sup>aa</sup>4 w vs. other groups,  $p < 0.05$ .

The anatomy of cortical and cancellous bone differs dramatically. The cancellous bone presents a large surface area upon which new repair bone can be deposited and highly vascularized marrow offers sufficient blood supply during fracture healing [20-22]. In our experiments we found two different patterns of bone formation, which differ from Uthoff finding. We observed that the cellular proliferation initially began at the fracture site between these vertical trabeculae, and the osteoblastic activity was promoted and formed the new woven bone on the surface of these vertical trabeculae. In time, this newly formed woven bone connected the pre-existing trabeculae on the two sides of the fracture gap. Moreover, we demonstrated that this type of bone formation could produce the lamella bone directly on the surface of pre-existing trabeculae. Furthermore, we observed that the activated mesenchymal-like cells differentiated into osteoblasts and formed the woven bone in the marrow tissue at the fracture site. This woven bone

formed an "island" like structure independently and then transformed into a lamellar structure through remodeling. These two different ways of bone formation occurred together to reunite the fragments and ensured that the trabeculae regained loading strength. No callus formation was found during the whole process of fracture healing.

Bone development occurs by two mechanisms, namely intramembranous bone formation and endochondral bone formation. These mechanisms also occur in fracture and osteotomy repair, with the specific mechanism dependent on the mechanical environment provided during repair [6, 20, 23]. With

intramembranous bone repair, mesenchymal cells differentiate along a pre-osteoblast to osteoblast line, whereas endochondral bone repair is characterized by the initial synthesis of cartilage followed by the endochondral sequence of bone formation. The terms intramembranous and endochondral refer to the tissue being replaced, not to the eventual bone synthesized, which is the same in both mechanisms [24, 25]. In our experiments, we observed that only the intramembranous repair had taken part in the process of fracture healing. The two different patterns of bone formation described above both belong to the intramembranous repair. The first pattern of bone formation, which was induced by the mesenchymal osteoblasts in the bone marrow of the fracture site, was the typical intramembranous repair. The second pattern occurred at the surface of pre-existing trabeculae to thicken the size of trabecular bone forming the lamellar bone and branch-like woven bone directly. This process shows a small difference from the classical

## Unique four stage healing pattern in cancellous fracture healing

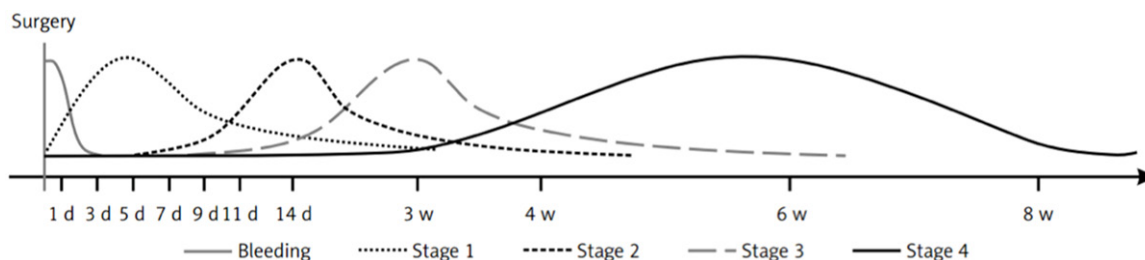


**Figure 11.** Stages of the extremity fracture healing process.

intramembranous bone formation in that osteo-progenitor cells of the endosteum partially induced the newly formed woven bone.

How can the process of direct fracture healing and indirect fracture healing be identified? To our knowledge, direct healing means the fracture is repaired by bone tissue directly including woven bone and lamella bone. Indirect healing means the fracture is repaired through fibrous tissue or cartilaginous tissue initially which were replaced by bone tissue subsequently. The classical “primary fracture healing” concept is that if the fracture is anatomically reduced and rigidly fixed, at the micrometric level, “osteonal” healing occurs. Osteoclasts create “cutting cones” and primarily cross the fracture site. This requires very high stability. More commonly, “secondary” fracture healing occurs and a larger mass of callus is created [6, 20, 21]. The secondary healing process of cortical bone can be divided into four stages: inflammation, soft callus formation, hard callus formation, and bone remodeling. However, in our study, we found that a three-stage model could explain the healing process of cancellous fracture healing: cell proliferation, woven bone formation, and remodeling. Compared with the “secondary healing” process, in our study, only a slight interruption to normal vascular function and a little distortion of the trabecular architecture were found during the first stage, but no hematoma development, osteo-necrosis or inflammation was detected. The reactions to fracture were limited to the area of cancellous bone and no callus formed by periosteum reaction was found. Compared with the process of “primary healing”, although we used strict anatomical reduction, the space between the trabecular bones still existed, and the fracture healed directly through intramembranous bone formation. The bone mass of the fracture site increased at first, then decreased. It seemed

that the “internal callus” was formed during the healing process, which remodeled into a normal structure. These findings indicate that the healing process of cancellous fracture is unique compared with the primary and secondary fracture healing of cortical bone.

The measurement of parameters of cancellous bone is one of the most important methods of evaluating cancellous fracture healing [11, 12]. To confirm our histology finding, we examined the parameters of proportions of cancellous bone by histomorphometry. In this study, we found that the BV/TV and Tb.N increased to reach a peak and Tb.Sp was minimal at 2 weeks postoperatively, while Tb.Th continued to increase. The increase of BV/TV in early phase was mainly induced by the newly formed immature trabeculae, which showed higher numbers, smaller size, and lower separation. We detected biomechanical changes during the fracture healing to observe the state of weight function of the fracture site. We found that the maximum load and maximum energy absorption were higher than the normal value at 2 weeks after surgery and reached a peak at 4 weeks. These data indicated that the cancellous fracture healed and gained functional healing at 4 weeks postoperatively, and the trabecular architecture was mature enough at this time point. At 6 weeks after surgery, the parameters of histomorphometry and biomechanics showed a slight decrease and then returned to a normal level. This might be induced by the high activity of bone remodeling at 6 weeks after surgery.

In our study, we did not observe obvious osteo-necrosis and bone resorption before 2 weeks. We observed that the osteoclasts and related absorption lacunae presented on the surface of newly formed woven bone at 2 weeks after surgery, while the BMU appeared on the sur-

## Unique four stage healing pattern in cancellous fracture healing

face of almost all the newly formed trabecular bone at the fracture site at 4 weeks and reached a peak at 6 weeks. These findings differ from the previous study, which indicated that the fracture healed directly at first and transformed to the mature structure through bone remodeling.

Clinically, the uniqueness of metaphysis cancellous bone healing has been confused with the diaphyseal cortical bone healing for decades. No specific theory has been hypothesized to explain the unique features of cancellous bone healing such as rapid healing and almost no hematoma formation in the fracture gap. In the current study, our data show that cancellous bone fracture healing reactions are limited within the range of cancellous bone and no callus formed by periosteum reaction can be found. Moreover, the bone mass of the fracture site experienced an increase at first and then decreased subsequently. Our finding indicates that the cancellous fracture healing applies to an over-production and carve-out fashion. In previous studies, osteoblast and osteoclast coordination played a pivotal role in this process. Thus, local application of a pharmaceutical agent targeting osteoblast or osteoclast cross-talk may elucidate a promising clinical effect. Wang and colleagues reported that NF $\kappa$ B signal suppresses the osteoblast function in osteoporosis pathology [26]. Together with our findings in the current study, local administration of an NK- $\kappa$ B specific inhibitor in the fracture gap during surgery holds great promise to enhance the cancellous fracture healing, especially in osteoporosis patients.

However, there are several limitations to this study. First, due to the lack of a transgenic large animal model, we were not able to develop our study to investigate the cell signaling and gene expression changes in cancellous fracture healing. Thus, we designed a similar cancellous fracture model animal based on mice, which enabled a stable gene knockout strain. Second, extensive further studies are required to identify the specific cell types observed in the current work that participate in cancellous fracture repair. Of what nature are these repair cells? What is the origin of these repair cells? How do they coordinate with one another? These questions require urgent answers to

elucidate the general mechanisms of the cancellous bone fracture.

In conclusion, we designed a new extremity fracture model according to modern orthopedic clinical principles to investigate the histological process of fracture healing in the rabbit. Our data demonstrate that the metaphysis cancellous fracture heals in a unique fashion, which can be divided into four histological stages. It differs from common primary or secondary cortical fracture healing. Histological analysis showed that the fracture healed directly through intramembranous repair and included two different patterns: one occurred in the marrow of the fracture site, while the other occurred on the surface of pre-existing trabeculae.

In addition to a small area of bleeding at the fracture site before three days, the entire fracture healing process can be divided into four stages in histology: the first was characterized by cellular activation and differentiation from immediately after surgery to 3 weeks; the second was characterized by the formation of woven bone or new trabeculae from 5 days to 4 weeks; the third was the transformation of newly formed woven bone into a lamellar structure from 9 days to 6 weeks; the fourth was the period of remodeling after 2 weeks and reached a peak at 6 weeks. All stages overlapped with one another (**Figure 11**). There was no obvious fibrous tissue or chondrification formed during the whole healing process. The data of bone histomorphometry and biomechanical analysis showed that the structural parameters and parameters of healing strength changed as a unimodal curve.

Our current study revealed the unique healing process of trabecular bone fracture, which significantly differs from that of cortical bone fractures. Clinically, this finding will lead to a more specialized comprehension of metaphysis cancellous bone fracture and will shed new light on the development of therapies accordingly.

### Disclosure of conflict of interest

None.

**Address correspondence to:** Dr. Yang Zhao, Department of Orthopaedics, Harbin 242 Hospital, 3

## Unique four stage healing pattern in cancellous fracture healing

Weijian Street, Pingfang District, Harbin 150000, Heilongjiang, China. E-mail: zyhrb242@sina.com

### References

- [1] Armocida F, Barfield WR and Hartssock LA. Conventional plate fixation of periarticular fractures. *J Surg Orthop Adv* 2009; 18: 163-169.
- [2] Lerner A and Stein H. Hybrid thin wire external fixation: an effective, minimally invasive, modular surgical tool for the stabilization of periarticular fractures. *Orthopedics* 2004; 27: 59-62.
- [3] Carr JB. Surgical techniques useful in the treatment of complex periarticular fractures of the lower extremity. *Orthop Clin North Am* 1994; 25: 613-624.
- [4] Mosekilde L, Ebbesen EN, Tornvig L and Thomsen JS. Trabecular bone structure and strength-remodelling and repair. *J Musculoskelet Neuronal Interact* 2000; 1: 25-30.
- [5] Nunamaker DM. Experimental models of fracture repair. *Clin Orthop Relat Res* 1998; S56-65.
- [6] Shapiro F. Bone development and its relation to fracture repair. The role of mesenchymal osteoblasts and surface osteoblasts. *Eur Cell Mater* 2008; 15: 53-76.
- [7] Rabie AB, Dan Z and Samman N. Ultrastructural identification of cells involved in the healing of intramembranous and endochondral bones. *Int J Oral Maxillofac Surg* 1996; 25: 383-388.
- [8] Charnley J and Baker SL. Compression arthrodesis of the knee; a clinical and histological study. *J Bone Joint Surg Br* 1952; 34-B: 187-199.
- [9] Jarry L and Uthoff HK. Differences in healing of metaphyseal and diaphyseal fractures. *Can J Surg* 1971; 14: 127-135.
- [10] Uthoff HK and Rahn BA. Healing patterns of metaphyseal fractures. *Clin Orthop Relat Res* 1981; 295-303.
- [11] Parfitt AM. Bone histomorphometry: proposed system for standardization of nomenclature, symbols, and units. *Calcif Tissue Int* 1988; 42: 284-286.
- [12] Zhang L, Takahashi HE, Inoue J, Tanizawa T, Endo N, Yamamoto N and Hori M. Effects of intermittent administration of low dose human PTH(1-34) on cancellous and cortical bone of lumbar vertebral bodies in adult beagles. *Bone* 1997; 21: 501-506.
- [13] Gomes LS and Volpon JB. Experimental physeal fracture-separations treated with rigid internal fixation. *J Bone Joint Surg Am* 1993; 75: 1756-1764.
- [14] Curtis R, Goldhahn J, Schwyn R, Regazzoni P and Suhm N. Fixation principles in metaphyseal bone—a patent based review. *Osteoporos Int* 2005; 16 Suppl 2: S54-64.
- [15] Helfet DL, Haas NP, Schatzker J, Matter P, Moser R and Hanson B. AO philosophy and principles of fracture management—its evolution and evaluation. *J Bone Joint Surg Am* 2003; 85-A: 1156-1160.
- [16] Duan C, Liu J, Yuan Z, Meng G, Yang X, Jia S, Zhang J and Chen S. Adenovirus-mediated transfer of VEGF into marrow stromal cells combined with PLGA/TCP scaffold increases vascularization and promotes bone repair in vivo. *Arch Med Sci* 2014; 10: 174-181.
- [17] Senel K, Baykal T, Seferoglu B, Altas EU, Baygutaalp F, Ugur M and Kiziltunc A. Circulating vascular endothelial growth factor concentrations in patients with postmenopausal osteoporosis. *Arch Med Sci* 2013; 9: 709-712.
- [18] Ishikawa M, Ito H, Kitaori T, Murata K, Shibuya H, Furu M, Yoshitomi H, Fujii T, Yamamoto K and Matsuda S. MCP/CCR2 signaling is essential for recruitment of mesenchymal progenitor cells during the early phase of fracture healing. *PLoS One* 2014; 9: e104954.
- [19] Kawakami Y, Li M, Matsumoto T, Kuroda R, Kuroda T, Kwon SM, Kawamoto A, Akimaru H, Mifune Y, Shoji T, Fukui T, Kurosaka M and Asahara T. SDF-1/CXCR4 axis in Tie2-lineage cells including endothelial progenitor cells contributes to bone fracture healing. *J Bone Miner Res* 2015; 30: 95-105.
- [20] Phillips AM. Overview of the fracture healing cascade. *Injury* 2005; 36 Suppl 3: S5-7.
- [21] Buckwalter JA and Cooper RR. Bone structure and function. *Instr Course Lect* 1987; 36: 27-48.
- [22] Fan W, Crawford R and Xiao Y. Structural and cellular differences between metaphyseal and diaphyseal periosteum in different aged rats. *Bone* 2008; 42: 81-89.
- [23] Kusuzaki K, Kageyama N, Shinjo H, Takeshita H, Murata H, Hashiguchi S, Ashihara T and Hirasawa Y. Development of bone canaliculi during bone repair. *Bone* 2000; 27: 655-659.
- [24] Einhorn TA. The cell and molecular biology of fracture healing. *Clin Orthop Relat Res* 1998; S7-21.
- [25] Schindeler A, McDonald MM, Bokko P and Little DG. Bone remodeling during fracture repair: The cellular picture. *Semin Cell Dev Biol* 2008; 19: 459-466.
- [26] Chang J, Wang Z, Tang E, Fan Z, McCauley L, Franceschi R, Guan K, Krebsbach PH and Wang CY. Inhibition of osteoblastic bone formation by nuclear factor-kappaB. *Nat Med* 2009; 15: 682-689.